



Published in final edited form as:

Am J Physiol Renal Physiol. 2006 February ; 290(2): F297–F305. doi:10.1152/ajprenal.00147.2005.

## Characterization of ammonia transport by the kidney Rh glycoproteins RhBG and RhCG

Don-On Daniel Mak<sup>1</sup>, Binh Dang<sup>2</sup>, I. David Weiner<sup>3,4</sup>, J. Kevin Foskett<sup>1</sup>, and Connie M. Westhoff<sup>2,5</sup>

<sup>1</sup>Department of Physiology, University of Pennsylvania School of Medicine, Philadelphia

<sup>2</sup>American Red Cross, Philadelphia, Pennsylvania

<sup>3</sup>Division of Nephrology, University of Florida College of Medicine, Gainesville

<sup>4</sup>Nephrology and Hypertension Section, North Florida/South Georgia Veterans Health System, Gainesville, Florida

<sup>5</sup>Department of Pathology and Laboratory Medicine, University of Pennsylvania School of Medicine, Philadelphia

### Abstract

The erythrocyte Rh-associated glycoprotein (RhAG) was recently found to mediate transport of ammonia/ammonium when expressed in *Xenopus laevis* oocytes and yeast *Saccharomyces cerevisiae*. Nonerythroid homologs, RhBG and RhCG, are expressed in the mammalian kidney connecting segment and the collecting duct, major sites of urinary ammonia secretion. This study characterizes the transport properties of murine RhBG and RhCG by ammonium analog [<sup>14</sup>C]methylamine (MA) uptake and two-electrode voltage clamping of *X. laevis* oocytes. Both RhBG and RhCG mediated transport of ammonia, but differed in affinity for substrate ( $K_m = 2.5$  and 10 mM, respectively). The rates of RhBG- and RhCG-mediated transport were sensitive to the concentration of the protonated MA species and were stimulated by extracellular alkalosis and inhibited by acidosis, suggesting a role for H<sup>+</sup> in the transport process. Whereas expression of RhBG or RhCG caused a small increase in plasma membrane conductance, [<sup>14</sup>C]MA uptake was not affected by depolarization of oocytes with 100 mM extracellular K<sup>+</sup> or by clamping the membrane potential between 0 and –100 mV, indicating that RhBG- and RhCG-mediated transport was independent of the membrane potential. These results strongly suggest that RhBG and RhCG transport ammonia by an electroneutral process that involves  $NH_4^+/H^+$  exchange resulting in net NH<sub>3</sub> trans-location. The polarized localization of RhBG and RhCG in kidney tubules and the different substrate affinities may enable these proteins to participate in transepithelial ammonia secretion and to therefore play an important role in whole animal acid-base regulation.

Copyright © 2005 by the American Physiological Society.

Address for reprint requests and other correspondence: C. M. Westhoff, American Red Cross, 700 Spring Garden St., Philadelphia, PA 19123 or Dept. of Pathology and Laboratory Medicine, Univ. of Pennsylvania, 510 Stellar Chance, Philadelphia, PA 19104 (westhoff@mail.med.upenn.edu and westhoffc@usa.redcross.org).

## Keywords

Rh proteins; Rh-associated proteins; ammonium

Recent studies have shed light on the biological function of the Rh family of proteins, which are named for the erythrocyte members that are well-known blood group antigens. These proteins have distant sequence similarity to transporters that function in ammonium acquisition in bacteria (SNYN, AMT), yeast (MEP), and plants (AMT). We recently reported that the erythrocyte Rh-associated glycoprotein (RhAG) mediates movement of ammonia/ammonium when expressed in *Xenopus laevis* oocytes (40) and in the yeast, *Saccharomyces cerevisiae* (41). Functional characterization of erythrocyte RhAG expressed in oocytes revealed transport to be independent of the membrane potential and Na<sup>+</sup> gradient, but it was dramatically affected by pH (40). Functional studies of RhAG expressed in a yeast mutant defective in ammonium transport, as well as in wild-type yeast, indicated that the transport was bidirectional and that the direction of substrate movement depended on the media pH (26, 41). Expression studies in both the oocyte (40) and yeast systems (41) indicated that RhAG mediates the transport of ammonia/ammonium, in a process that is influenced by the H<sup>+</sup> gradient across the membrane.

The nonerythroid homologs, designated RhBG and RhCG, are expressed in kidney, liver, brain, gastrointestinal tract, and skin (15, 22, 23, 39). In the kidney, RhBG and RhCG have been localized to the basolateral and apical membranes, respectively, in the collecting segment and collecting duct (33, 39), major sites of transepithelial ammonia/ammonium transport. In the intestinal tract, RhBG and RhCG are expressed in a similar polarized fashion in the duodenum and other regions of small and large intestine, other important sites for transepithelial ammonia transport (15). Recent studies in a mouse collecting duct cell line (mIMCD-3), which expresses basolateral RhBG and apical RhCG, revealed that both basolateral and apical ammonia/ammonium movement in these cells had characteristics of a protein-mediated transport process (13, 14). The transport activity was distinct from known potassium or sodium transporters, was independent of the membrane potential, and was stimulated by establishment of a transmembrane proton gradient, consistent with the behavior of erythrocyte RhAG expressed in heterologous cells (40). These studies suggested that the kidney RhBG and RhCG proteins may function in transepithelial movement of ammonia/ammonium.

In mammals, renal ammonium metabolism and transport are critical for whole animal acid-base balance. Ammonium ions are the primary component of net acid excretion under basal conditions and changes in renal ammonia metabolism and transport comprise the predominant renal response to metabolic acidosis (10, 21). Total ammonia secretion along the length of the collecting tubule has been previously thought to occur by passive NH<sub>3</sub> diffusion. However, the recent observations concerning the function and localization of Rh glyco-proteins suggest that ammonia secretion may possibly be mediated by members of the Rh family of proteins.

We have therefore undertaken experiments to characterize the possible ammonia/ammonium transport activity of the nonerythroid Rh glycoproteins, RhBG and RhCG. Each protein was

expressed in *X. laevis* oocytes and functionally characterized utilizing two approaches: uptake of the ammonium analog [<sup>14</sup>C]methylamine (MA) and two-electrode voltage clamp (TEV) to assess the corresponding changes in membrane conductance, current, and reversal potential resulting from expression of the proteins in *X. laevis* oocytes.

## MATERIALS AND METHODS

### Constructs

Mouse kidney RhCG cDNA was obtained from a murine inner medullary collecting duct (mIMCD) cell line (ATCC), and mouse RhBG cDNA was obtained from a kidney Quick-Clone cDNA library (Clontech, Palo Alto, CA) by PCR with primers specific for the 5'- and 3'-regions of the published cDNAs. These were verified by sequencing, and cDNAs were cloned into the oocyte expression vector pBF (provided by F. Ashcroft, Oxford, UK). Cloning and propagation of plasmids followed standard procedures. Capped cRNA was synthesized with SP6 RNA polymerase from the linearized plasmid DNA with mMessage mMachine (Ambion, Austin, TX).

### Oocyte injection

Stage V and VI defolliculated oocytes obtained as described (16) were injected with 23–34 nl (1 µg/µl) of cRNA, or water for control, and placed in individual wells in 96-well plates containing 200 µl SOS containing (in mM) 100 NaCl, 2 KCl, 1.8 CaCl<sub>2</sub>, 1 MgCl<sub>2</sub>, 10 HEPES, pH 7.6, 200 mosM with 2.5 mM Na pyruvate and 100 µg/ml of gentamicin at 16°C. Oocytes were tested 3 days postinjection.

### Western analysis

Recombinant protein expression in oocytes was analyzed as previously described (40). Western blots were probed with rabbit polyclonal anti-peptide antibodies to mouse RhBG and mouse RhCG (37, 39) and visualized with secondary horseradish peroxidase-conjugated, anti-rabbit IgG followed by ECL chemiluminescence (Amersham, Arlington Heights, IL).

### MA flux assay

Radiolabeled [<sup>14</sup>C]methylammonium ( $CH_3NH_3^+$ ) (ICN, Irvine, CA) flux measurements were performed as described in detail previously (40). Briefly, six to eight oocytes were placed in 200 µl SOS uptake buffer containing 1 µCi/ml [<sup>14</sup>C]MA (20 µM) and various concentrations of unlabeled MA. For all experiments, radio-tracer uptake was stopped by washing the oocytes six times with 1 ml of ice-cold unlabeled uptake buffer. Oocytes were then solubilized in 200 µl of 5% SDS and analyzed for radioactivity by liquid scintillation counting. In all experiments, water-injected control oocytes were evaluated in parallel, and uptake by controls was subtracted from that observed in test oocytes. Flux assay data were analyzed with Igor Pro software (Wavemetrics, Lake Oswego, OR). Initial uptake rates were determined from slopes of linear fits to uptake measured over 15 to 30 min, during which efflux was considered negligible. Apparent EC<sub>50</sub> ( $K_m$ ) and  $V_{max}$  values were derived by

fitting experimental data with a simple Michaelis-Menten or Hill equation using Igor-Pro software with a nonlinear, least-squares fitting algorithm.

### TEV experiments

TEV (16) was used to measure membrane currents, conductance, and voltage in cRNA-injected or water-injected control oocytes 3 days postinjection, while the oocytes were perfused with a solution containing (in mM) 96 NaCl, 2 KCl, 1 CaCl<sub>2</sub>, 1.8 MgCl<sub>2</sub>, 5 HEPES, pH 7.5, or with solutions containing (in mM) 0.5, 1, 5, or 10 NH<sub>4</sub>Cl or MAcl, with correspondingly lower concentrations of NaCl to maintain the same osmolarity as detailed previously (40). The applied transmembrane potential ( $V_m$ ) was ramped from  $-90$  to  $+50$  mV every 10 s. Transmembrane current ( $I_m$ ) and  $V_m$  were digitized at 1 kHz during the voltage ramps. In data analysis with Igor Pro software, a fifth-order polynomial was fitted to the raw, monotonically increasing  $I_m$ - $V_m$  data from each voltage ramp. The whole oocyte membrane conductance and the reversal potential ( $V_{rev}$ ) were evaluated simultaneously as the slope ( $dI_m/dV_m$ ) and the  $x$ -intercept of the polynomial, respectively.

### [<sup>14</sup>C]MA flux assay under voltage clamp

Individual oocytes were voltage clamped to either  $-100$  or to  $0$  mV as for conventional TEV experiments. In each experiment, an oocyte was allowed to equilibrate for 3–5 min in uptake buffer without MA, and then an equal volume of uptake buffer containing  $2\times$  MA (radioactive and unlabeled) was added. Oocyte membrane integrity was monitored visually and by whole oocyte membrane conductance measurements during the experiment. After the flux uptake period (15 min), cold flux buffer was perfused by flow through the bath to remove extracellular radioactivity. The electrodes were then removed, and the oocyte was analyzed for radioactive uptake, as above. Uptake of MA under voltage-clamp conditions was compared with flux uptake in oocytes that were impaled with TEV microelectrodes but were allowed to remain at resting potential ( $-30$  to  $-50$  mV) without voltage clamp.

### Data analysis

The statistical significance of experimental results was evaluated by two-tailed  $t$ -test.  $P$  values  $<0.05$  were considered significant. Data are plotted in Figs. 1–9 as arithmetic means  $\pm$  SEM;  $n$  is reported as the number of different assays.

## RESULTS

By convention, we will use the term “ammonia” to refer to the sum of  $NH_4^+$  and  $NH_3$ , “ammonium” or  $NH_4^+$  to indicate the protonated form of the molecule, and “ $NH_3$ ” when referring to the unprotonated molecular species.

### RhBG and RhCG mediate uptake of MA

To begin testing the hypothesis that RhBG and RhCG mediate movement of total ammonia and to characterize that transport, we expressed the nonerythroid Rh glycoproteins in *X. laevis* oocytes. cRNA for RhBG or RhCG was microinjected into oocytes and expression was monitored at 72 h after injection. Protein expression was detected after SDS-PAGE

separation and immunoblotting with rabbit anti-peptide antibodies specific for RhBG or RhCG (39). RhBG migrated at ~52 kDa (Fig. 1A, *inset*), and RhCG at ~58 kDa (Fig. 1B, *inset*), consistent with the reported molecular weights of these glycoproteins in mouse tissues (37, 39). The detected proteins were absent in water-injected control oocytes.

We previously showed that the radioactive analog tracer methylamine,  $[^{14}\text{C}] \text{CH}_3\text{NH}_3^+$  ( $\text{MA}^+/\text{MA}$ ), which has been used to study ammonium transport in yeast and plants (20, 28, 32, 34), had the same relative affinity as  $\text{NH}_3/\text{NH}_4^+$  for the RhAG transport pathway (40). Therefore, we used the uptake of  $[^{14}\text{C}]\text{MA}$  in cRNA-injected oocytes as a measure of  $\text{NH}_3/\text{NH}_4^+$  transport mediated by RhBG and RhCG. Expression of either mouse RhBG or mouse RhCG enhanced the rate of  $\text{MA}^+/\text{MA}$  uptake compared with that seen in the water-injected controls by two- to threefold over controls at 500  $\mu\text{M}$  substrate concentration (Fig. 1). Uptake was saturable at 1 h (not shown), which is compatible with the uptake being a carrier-mediated process. In all subsequent flux experiments, water-injected control oocytes were evaluated, and the uptake reported was the uptake by the RhBG- or RhCG-expressing oocytes less the uptake by the control water-injected oocytes examined in parallel.

### Effects of ammonium, organic ions, and inhibitors on MA transport

To confirm that  $\text{NH}_3/\text{NH}_4^+$  is the actual substrate for RhBG and RhCG transport, competitive inhibition experiments were performed by measuring  $\text{MA}^+/\text{MA}$  uptake in the presence of varying concentrations of  $\text{NH}_4\text{Cl}$ . Uptake by RhBG and RhCG was significantly inhibited by ammonia (Fig. 2A). Differences in the concentration of ammonia required to inhibit RhBG- and RhCG-mediated  $\text{MA}^+/\text{MA}$  uptake suggest that these proteins differ in their affinity for substrate. An inhibitory Hill equation fit to the data gave an  $\text{IC}_{50}$  for  $\text{MA}^+/\text{MA}$  transport inhibition by  $\text{NH}_4\text{Cl}$  of ~0.5 mM for RhBG and ~2.9 mM for RhCG and a Hill coefficient of 1.4 for both.

Inhibition of  $\text{MA}^+/\text{MA}$  uptake was specific for ammonia as uptake was not affected by 10- to 20-fold higher concentrations of the amine containing compounds TMA, TEA, urea, or glutamine (Fig. 2B). We also measured uptake in the presence of inhibitors of potential ammonia transporters. Amiloride (1 mM), an inhibitor of  $\text{Na}^+/\text{H}^+$  exchangers, did not significantly alter RhBG- or RhCG-mediated  $\text{MA}^+/\text{MA}$  uptake (Fig. 2C). Although  $\text{NH}_4^+$  has approximately the same ionic radius as hydrated  $\text{K}^+$  and can substitute for  $\text{K}^+$  on several transporters (18, 19, 38), we observed no inhibitory effect of  $\text{K}^+$  transporter inhibitors bumetanide or ouabain (Fig. 2C). Unfortunately, no inhibitors of the yeast, plant, or bacterial ammonium transporters have been reported to date. We tested flufenamate (FFA) because it was reported to partially inhibit the membrane depolarization seen in oocytes when they are suspended in high concentrations (20 mM) of ammonium (4). However, FFA had no effect on RhBG- or RhCG-mediated MA uptake (Fig. 2C).

### Transport kinetics

To determine the kinetics of transport, the rates of  $\text{MA}^+/\text{MA}$  uptake were measured with increasing concentrations of substrate ranging from 20  $\mu\text{M}$  to 50 mM. When fitted with a Hill equation, the Hill coefficient was  $0.9 \pm 0.1$ , suggesting a lack of transporter

cooperativity. Thus the data were well fitted with a Michaelis-Menten equation (Fig. 3, A and B). The  $EC_{50}$  ( $K_m$ ) for RhBG was  $2.5 \pm 0.5$  mM, whereas the  $EC_{50}$  ( $K_m$ ) for RhCG was  $10 \pm 2$  mM. These data suggest that RhBG and RhCG may function as low-affinity, high-capacity transporters and indicate that RhBG has a higher affinity for  $MA^+/MA$  than RhCG.

### Transport is pH sensitive and driven predominantly by protonated substrate concentration

We previously showed that RhAG-mediated uptake was pH sensitive, being enhanced at alkaline extracellular pH and inhibited at acid extracellular pH (40), and that a transmembrane proton gradient appeared to influence the direction of substrate transport (41). To ascertain whether MA uptake by RhBG and RhCG was also pH sensitive, uptake in buffers with pH ranging from 6.5 to 8.5 was measured. The rate of MA uptake in RhBG and RhCG cRNA-injected oocytes increased at alkaline pH values in the presence of constant total methylamine concentration (Fig. 4). Because increasing the pH of the uptake buffer causes an increase in the concentration of the unprotonated molecule in the solution (10-fold increase in unprotonated MA concentration for every unit rise in pH according to the Henderson-Hasselback equation), it is possible that the higher uptake rate observed in more alkaline extracellular conditions is simply due to the increase in the concentration of unprotonated MA as the substrate transported. If the transport rate is determined only by the concentration of the unprotonated species, the rate would be predicted to increase 10-fold as pH was increased from 7.5 to 8.5. However, the observed increase was threefold or less, arguing against a simple response to the change in concentration of the unprotonated species.

To further ascertain whether the enhanced uptake rate at higher pH values was the result of an increase in the concentration of the unprotonated species, with the unprotonated species driving the transport rate, we measured uptake in buffers that contained equivalent concentrations of unprotonated MA (0.38, 7.6, or 11.4  $\mu$ M), but that had a 10-fold difference in the concentration of protonated  $MA^+$  (Fig. 5). If the transport rate depends only on the concentration of the unprotonated molecule, we would expect the uptake rate in the presence of a given concentration of unprotonated species to be equivalent, regardless of the concentration of protonated ion present. However, uptake in both the RhBG and RhCG cRNA-injected oocytes differed significantly in different concentrations of  $MA^+$  in the presence of a fixed concentration of the unprotonated substrate (Fig. 5). Indeed, in the presence of subsaturating concentrations of  $MA^+$ , the uptake rate is proportional to the concentration of protonated  $MA^+$  (Fig. 5, A and B). These data indicate that the rate of transport is affected predominantly by the concentration of the protonated species.

### Two-electrode voltage-clamp experiments

Two-electrode voltage-clamp experiments were undertaken to determine the effects of RhBG- and RhCG-mediated transport on membrane conductance, current, and reversal potential in the presence of various concentrations of  $NH_4Cl$  in the extracellular bath solution. We measured  $NH_4Cl$ - and methylamine-induced currents over a wide range of substrate concentrations and voltages to compare the magnitudes of membrane conductance and depolarization in RhBG- or RhCG-expressing oocytes to the water-injected controls.

In water-injected oocytes not expressing RhBG or RhCG, high concentrations of extracellular  $\text{NH}_4\text{Cl}$  (~10 mM) increased membrane conductance and depolarized the oocytes (our unpublished observations and Ref. 2). This endogenous  $\text{NH}_4\text{Cl}$ -dependent conductance complicates efforts to observe specific RhBG- or RhCG-mediated  $\text{NH}_4\text{Cl}$ -dependent transport in oocytes in the presence of high (>5 mM)  $\text{NH}_4\text{Cl}$  concentrations. The endogenous  $\text{NH}_4\text{Cl}$ -dependent conductance is substantially smaller in the presence of the low  $\text{NH}_4\text{Cl}$  concentrations (0.5–1 mM) at which RhBG and RhCG transport  $\text{MA}/\text{MA}^+$  effectively, as shown in the uptake studies (Fig. 3). Therefore, we looked for possible RhBG- or RhCG-mediated  $\text{NH}_4\text{Cl}$ -dependent transmembrane conductances in the presence of 0.5 to 1 mM  $\text{NH}_4\text{Cl}$ .

In a representative TEV experiment (Fig. 6), the transmembrane current  $I_m$  in an RhBG-injected oocyte (dots) was monitored at various applied potentials,  $V_m$ , according to a voltage ramp protocol. From the fits (continuous curve) to the  $I_m$ - $V_m$  data, the whole cell current (Fig. 6B), the transmembrane conductance (Fig. 6C) at  $V_m = -50$  mV, and the reversal potential (Fig. 6D) of the oocyte were evaluated simultaneously while the oocyte was continuously perfused with bath solutions containing various concentrations of  $\text{NH}_4\text{Cl}$ .

Cumulative results of multiple TEV experiments using water-injected and RhBG and RhCG cRNA-injected oocytes perfused with 1 mM  $\text{NH}_4\text{Cl}$  are shown in Fig. 7. Expression of RhBG or RhCG induced small changes in membrane conductance and reversal potential in the absence of  $\text{NH}_4\text{Cl}$  (open bars in Fig. 7, A and C). The addition of 1 mM  $\text{NH}_4\text{Cl}$  to the bath solution elicited slight depolarization (Fig. 7C) and small increases in the conductance (Fig. 7A) of water-injected controls, as well as RhBG and RhCG cRNA-injected oocytes, with greater conductance increase in RhBG cRNA-injected oocytes than that observed for controls (Fig. 7B). Higher bath  $\text{NH}_4\text{Cl}$  concentrations (5, 10, and 20 mM) caused substantial depolarization and conductance increase (compared with 0 mM  $\text{NH}_4\text{Cl}$ ) in all oocytes (RhBG, RhCG cRNA- or water-injected) with no significant difference between them (data not shown).

### Transport is not dependent on membrane potential

The above results indicate that Rh glycoprotein expression may be associated with enhanced membrane conductance. It is not always possible to distinguish, using TEV measurements alone, between transport of specific ions via exogenous proteins and activation of an endogenous conductance. Upregulation of endogenous conductances as a result of expression of recombinant membrane proteins is not uncommon in oocytes (3, 5, 31, 35, 36). Therefore, to determine whether RhBG or RhCG expression in oocytes results in enhanced movement of charged  $\text{MA}^+$  or  $\text{NH}_4^+$  across the membrane, we investigated the dependence of  $\text{MA}/\text{MA}^+$  uptake on the membrane potential. First, we replaced the  $\text{Na}^+$  in the uptake buffer (100 mM  $\text{Na}^+$ , 1 mM  $\text{K}^+$ ) with  $\text{K}^+$  (100 mM  $\text{K}^+$ , 1 mM  $\text{Na}^+$ ) so that the oocytes were nearly completely depolarized (40). Uptake of radioactive  $\text{MA}^+/\text{MA}$  was unaffected by this ionic replacement (Fig. 8A). This suggests that  $\text{MA}^+/\text{MA}$  uptake is not electrogenic, and furthermore, that uptake is independent of the transmembrane  $\text{Na}^+$  gradient.

To confirm that transport was insensitive to membrane potential, uptake was measured in oocytes voltage-clamped at 0 or  $-100$  mV, and the results were compared with those obtained in unclamped oocytes (Fig. 8B). There were no significant differences in  $MA^+/MA$  uptake in RhBG- and RhCG-expressing oocytes when the membrane was clamped at these voltages. Taken together, these results indicate that transport mediated by the Rh glycoproteins is electroneutral.

## DISCUSSION

The discoveries that erythroid RhAG mediates transport of ammonia/ammonium when expressed in *X. laevis* oocytes (40) and yeast (26, 41) and that the kidney homologs, RhBG and RhCG, show polarized expression in the collecting segment and collecting duct (39) suggest a role for these homologs in transepithelial transport of ammonia/ammonium by the kidney. Movement of ammonia ions in the kidney collecting duct has been thought to occur by passive diffusion of  $NH_3$ . The possibility that this process may be protein mediated via members of the Rh-associated glycoprotein family motivated our efforts to characterize the transport activity of the kidney homologs, as previously done to characterize erythrocyte RhAG.

We found that both RhBG and RhCG mediated the transport of the ammonia/ammonium analog, MA, in a process that was competitively inhibited specifically by  $NH_4Cl$ , but not by other amine compounds. Kinetic measurements revealed that RhBG had a higher affinity for  $MA/MA^+$  than RhCG. This observation is consistent with differences in the local  $NH_3/NH_4^+$  concentration in the collecting duct in the kidney where these proteins are localized (Fig. 9). RhCG is expressed on the apical cell surface facing the lumen (39) where the concentration of ammonium can reach 200 mM. In contrast, RhBG is localized to the basolateral surface facing the interstitium, where concentrations are significantly lower ( $<5$  mM) (21). Thus the substrate affinities of RhBG and RhCG may be specific adaptations that enable these proteins to facilitate the vectorial transport of ammonia in the collecting duct in locations with disparate substrate concentrations.

Our data show that RhBG- and RhCG-mediated uptake of  $MA/MA^+$  was sensitive to the proton ( $H^+$ ) concentration in the extracellular buffer. Uptake was inhibited at acidic pH and enhanced at alkaline pH. Importantly, the enhanced uptake at alkaline pH was not due to increased concentration of unprotonated MA. In contrast, uptake rates in the presence of an equivalent concentration of unprotonated MA differed dramatically depending on the amount of protonated  $MA^+$  present, indicating that RhBG and RhCG respond to protonated substrate concentration in the extracellular medium. Nevertheless, the concentration of protonated  $MA^+$  was not the sole determinant of the rate of transport. Rather, the magnitude and direction of the  $H^+$  gradient also contribute to the rate of transport. Taken together, these data suggest a mechanism involving  $NH_4^+$  and its movement across the plasma membrane by exchange with intracellular protons, resulting in electroneutral transport.

The membrane conductance monitored in TEV experiments was higher in the oocytes expressing RhBG and RhCG than in control ones, both in the absence as well as presence of extracellular  $NH_4Cl$ . The nature of this conductance is not known, but our results suggest



that it is unrelated to the Rh glycoprotein-mediated mechanism that transports MA. The TEV results revealed that oocytes have an endogenous  $\text{NH}_4\text{Cl}$ -stimulated conductance even in the absence of RhBG/RhCG expression. The elevated conductance observed in RhBG/RhCG-expressing oocytes may reflect upregulation of this endogenous conductance.

Several groups have also reported enhanced conductance in RhBG (24, 30) or RhCG (1) cRNA-injected oocytes. Observed intracellular acidification, transmembrane currents, and cell depolarization in RhBG cRNA-injected oocytes exposed to 5 mM  $\text{NH}_4\text{Cl}$  led Nakhoul et al. (30) to conclude that RhBG mediates electrogenic transport of protonated  $\text{NH}_4^+$  across the plasma membrane. In contrast, Ludwig (24) observed a transient intracellular alkalization but also found enhanced inward currents in voltage-clamped, RhBG cRNA-injected oocytes perfused with 500  $\mu\text{M}$   $\text{NH}_4\text{Cl}$ . Enhanced inward currents were also observed in voltage-clamped RhCG cRNA-injected oocytes (1). The results of these studies are reminiscent of the enhanced conductance observed in the experiments reported here. However, our direct measurements of substrate uptake in voltage-clamped oocytes now strongly indicate that the ammonia-stimulated conductance is distinct from the transport mechanism that mediates translocation of MA/MA<sup>+</sup> by RhBG and RhCG. In agreement, Ludwig (24) also concluded that inward currents observed were not directly associated with the mechanism that mediates RhBG transport. Of note, many studies have observed the upregulation of endogenous oocyte conductances in response to recombinant protein expression (3, 5, 31, 35, 36). Because TEV conductance and current measurements in oocytes can be confounded by movement of ions other than those under study, we used radioactive labeled MA to directly monitor substrate movement across the membrane in RhBG- and RhCG-expressing oocytes under voltage-clamp conditions. Importantly, MA uptake was unaffected by large changes in the potential difference across the plasma membrane. These results strongly suggest that Rh-associated glycoprotein-mediated ammonia uptake is intrinsically an electroneutral transport process. Taken together with the evidence that the transport process involves  $\text{NH}_4^+$  and an oppositely directed  $\text{H}^+$  gradient, we conclude that both RhBG and RhCG expressed in *X. laevis* oocytes mediate electroneutral transport of  $\text{NH}_4^+$  and  $\text{H}^+$  which results in the net transport of  $\text{NH}_3$  across the plasma membrane of the cell.

Members of the Amt/MEP/Rh family of proteins, to which RhBG and RhCG belong, are expressed in a broad range of organisms, from bacteria and yeast to plants and mammals. The structure of *E. coli* AmtB has recently been solved by two groups using X-ray crystallography (17, 42). The structure reveals that the bacterial protein transports uncharged  $\text{NH}_3$  via a unique mechanism. AmtB contains an extracellular vestibule that recruits  $\text{NH}_4^+$  cations, but the hydrophobic pore through the membrane is narrow. The  $\text{NH}_4^+$  is stripped of a proton in the vestibule, enabling uncharged  $\text{NH}_3$  to pass through the pore via weak interactions with hydrogen bond donors that line the pore. A proton is released back to the extracellular aqueous phase during the process. Conversely,  $\text{NH}_3$  is re protonated at the intracellular face of the channel. The net result is  $\text{NH}_4^+$  transport in exchange for  $\text{H}^+$ . The mechanisms regarding  $\text{NH}_3/\text{NH}_4^+$  transport by AmtB inferred from analyses of the crystal structures are entirely consistent with our experimental data showing that the mammalian

Rh-associated glycoproteins (RhAG, RhBG, and RhCG) mediate electroneutral transport with net transfer of  $\text{NH}_3$ . The extracellular alkaline pH stimulation and transmembrane proton gradient sensitivity seen with the Rh-associated glycoproteins are consistent with the requirement for transfer of a proton to the extracellular aqueous phase concurrent with movement of  $\text{NH}_3$  across the membrane. The structures support our original hypothesis that the transport mechanism involves exchange of  $\text{NH}_4^+$  for  $\text{H}^+$  (40), although the molecular details are distinct from those of a  $\text{NH}_4^+/\text{H}^+$  exchanger mechanism.

Nevertheless, the relevance of the AmtB structure for the mechanism of  $\text{NH}_3$  transport by Rh-associated glycoproteins remains to be more fully established. Notably, in contrast to the mammalian Rh-associated glycoproteins, pH has not been observed to affect uptake by the bacterial (29), plant (25), or yeast (27) proteins. Thus the mechanism of transport by the mammalian proteins may differ from the plant, bacterial, and yeast transporters. It has been proposed that the bacterial and plant transporters require a membrane potential gradient (28, 29, 32). However, because this conclusion was based on the use of protonophores to dissipate membrane potential, this interpretation may have been confounded by the fact that the membrane potential in these organisms is maintained by proton pumps. Thus an alternative explanation for those observations is that protonophores interfered with uptake because they eliminated the proton gradient required for uptake.

In the kidney, RhBG and RhCG may function to mediate transepithelial transfer of  $\text{NH}_3/\text{NH}_4^+$  from the interstitium to the lumen in the collecting duct. In support, mIMCD grown on permeable support membranes demonstrate both apical and basolateral plasma membrane ammonia-inhibitable [ $^{14}\text{C}$ ]MA uptake, compatible with a transporter-mediated apical and basolateral membrane process (13, 14). The transport kinetics measured in the mIMCD cells were very similar to those obtained in the oocyte experiments reported here. Figure 9 is a diagrammatic representation of the medullary collecting duct showing the location of RhBG and RhCG and indicating the approximate local concentration of ammonia (both  $\text{NH}_4^+$  and  $\text{NH}_3$ ) and the pH. The basolateral pH may vary along the collecting duct, progressing from slightly more acidic than systemic pH to slightly more alkaline (7, 8, 11). Extracellular ammonia concentrations also vary along the length of the collecting duct (reviewed in Ref. 6) and the collecting duct luminal  $\text{NH}_4^+$  concentration can exceed 200 mM. However, our study indicates that RhBG and RhCG transport net  $\text{NH}_3$  across the plasma membrane through an electroneutral process involving  $\text{NH}_4^+/\text{H}^+$  exchange. This movement of net  $\text{NH}_3$  is determined by the transmembrane concentration gradients of  $\text{NH}_4^+$  and  $\text{H}^+$ . The net transport of  $\text{NH}_3$  mediated by RhBG and RhCG from the interstitium through the epithelial cell cytoplasm to the collecting duct lumen proceeds down the  $\text{NH}_3$  concentration gradient (from ~50–90 through 50 to 7–35  $\mu\text{M}$ ) and therefore requires no energy input. The rates of RhBG- and RhCG-mediated transport are determined by the pH and  $\text{NH}_4^+$  concentrations of the interstitium, epithelial cell cytoplasm, and collecting duct lumen, which are regulated by various cellular mechanisms. Indeed, transepithelial ammonia secretion rate in the collecting duct is known to be determined by both the ammonia concentration and the pH gradient (9, 12), and increasing luminal  $\text{H}^+$  concentration stimulates transepithelial ammonia secretion.

In mammals,  $NH_3/NH_4^+$  secretion is critical for acid-base balance. The localization of RhBG and RhCG to the connecting segment and collecting duct, the final sites of renal acid secretion, positions them to affect acid-base regulation. The causes of some forms of distal renal tubular acidosis, an inherited disorder affecting acid-base transport in the renal collecting duct, have not yet been uncovered, making RhCG and RhBG prime targets for investigation. Functional studies of the kidney and erythrocyte Rh-associated proteins promise to contribute to understanding the role of these proteins in ammonia/ammonium elimination.

## Acknowledgments

### GRANTS

This work was supported by National Institutes of Health Grants DK-02751 to C. M. Westhoff and DK-45788 and NS-47624 and the Department of Veterans Affairs Merit Review Program (to I. D. Weiner).

## REFERENCES

1. Bakouh N, Benjelloun F, Hulin P, Brouillard F, Edelman A, Cherif-Zahar B, Planelles G.  $NH_3$  is involved in the  $NH_4^+$  transport induced by the functional expression of the human Rh C glycoprotein. *J Biol Chem.* 2004; 279:15975–15983. [PubMed: 14761968]
2. Boldt M, Burckhardt G, Burckhardt B.  $NH_4^+$  conductance in *Xenopus laevis* oocytes. III. Effect of  $NH_3$ . *Pflügers Arch.* 2003; 446:652–657. [PubMed: 12827361]
3. Broer S, Schuster A, Wagner CA, Broer A, Forster I, Biber J, Murer H, Werner A, Lang F, Busch AE. Chloride conductance and Pi transport are separate functions induced by the expression of NaPi-1 in *Xenopus* oocytes. *J Membr Biol.* 1998; 164:71–77. [PubMed: 9636245]
4. Burckhardt MC, Fromter E. Pathways of  $NH_3/NH_4^+$  permeation across *Xenopus laevis* oocyte cell membrane. *Pflügers Arch.* 1992; 420:83–86. [PubMed: 1372714]
5. Buyse G, Voets T, Tytgat J, De Greef C, Droogmans G, Nilius B, Eggermont J. Expression of human pICln and ClC-6 in *Xenopus* oocytes induces an identical endogenous chloride conductance. *J Biol Chem.* 1997; 272:3615–3621. [PubMed: 9013613]
6. DuBose TD Jr, Good DW, Hamm LL, Wall SM. Ammonium transport in the kidney: new physiological concepts and their clinical implications. *J Am Soc Nephrol.* 1991; 1:1193–1203. [PubMed: 1932632]
7. DuBose TD Jr, Pucacco LR, Lucci MS, Carter NW. Micropuncture determination of pH,  $PCO_2$ , and total  $CO_2$  concentration in accessible structures of the rat renal cortex. *J Clin Invest.* 1979; 64:476–482. [PubMed: 37258]
8. Filho EM, Malnic G. pH in cortical peritubular capillaries of rat kidney. *Pflügers Arch.* 1976; 363:211–217. [PubMed: 8760]
9. Flessner MF, Wall SM, Knepper MA. Ammonium and bicarbonate transport in rat outer medullary collecting ducts. *Am J Physiol Renal Fluid Electrolyte Physiol.* 1992; 262:F1–F7.
10. Frank AE, Wingo CS, Andrews PM, Ageloff S, Knepper MA, Weiner ID. Mechanisms through which ammonia regulates cortical collecting duct net proton secretion. *Am J Physiol Renal Physiol.* 2002; 282:F1120–F1128. [PubMed: 11997329]
11. Good DW, Caflisch CR, DuBose TD Jr. Transepithelial ammonia concentration gradients in inner medulla of the rat. *Am J Physiol Renal Fluid Electrolyte Physiol.* 1987; 252:F491–F500.
12. Hamm LL, Trigg D, Martin D, Gillespie C, Buerkert J. Transport of ammonia in the rabbit cortical collecting tubule. *J Clin Invest.* 1985; 75:478–485. [PubMed: 3973014]
13. Handlogten ME, Hong SP, Westhoff CM, Weiner ID. Apical ammonia transport by the mouse inner medullary collecting duct cell (mIMCD-3). *Am J Physiol Renal Physiol.* 2005; 289:F347–F358. [PubMed: 15798090]

14. Handlogten ME, Hong SP, Westhoff CM, Weiner ID. Basolateral ammonium transport by the mouse inner medullary collecting duct cell (mIMCD-3). *Am J Physiol Renal Physiol.* 2004; 287:F628–F638. [PubMed: 15149971]
15. Handlogten ME, Hong SP, Zhang L, Vander AW, Steinbaum ML, Campbell-Thompson M, Weiner ID. Expression of the ammonia transporter proteins Rh B glycoprotein and Rh C glycoprotein in the intestinal tract. *Am J Physiol Gastrointest Liver Physiol.* 2005; 288:G1036–G1047. [PubMed: 15576624]
16. Jiang Q, Mak D, Devidas S, Schwiebert EM, Bragin A, Zhang Y, Skach WR, Guggino WB, Foskett JK, Engelhardt JF. Cystic fibrosis transmembrane conductance regulator-associated ATP release is controlled by a chloride sensor. *J Cell Biol.* 1998; 143:645–657. [PubMed: 9813087]
17. Khademi S, O'Connell J III, Remis J, Robles-Colmenares Y, Miercke LJ, Stroud RM. Mechanism of ammonia transport by Amt/MEP/Rh: structure of AmtB at 1.35 Å. *Science.* 2004; 305:1587–1594. [PubMed: 15361618]
18. Kinne R, Kinne-Saffran E, Shutz H, Scholermann B. Ammonium transport in medullary thick ascending limb of rabbit kidney: involvement of the Na<sup>+</sup>, K<sup>+</sup>, Cl<sup>-</sup>-cotransporter. *J Membr Biol.* 1986; 94:279–284. [PubMed: 3560204]
19. Kinsella JL, Aronson PS. Interaction of NH<sub>4</sub><sup>+</sup> and Li<sup>+</sup> with the renal microvillus membrane Na<sup>+</sup>-H<sup>+</sup> exchanger. *Am J Physiol Cell Physiol.* 1981; 241:C220–C226.
20. Kleiner D. The transport of NH<sub>3</sub> and NH<sub>4</sub><sup>+</sup> across biological membranes. *Biochim Biophys Acta.* 1981; 639:41–52. [PubMed: 7030397]
21. Knepper MA, Packer R, Good DW. Ammonium transport in the kidney. *Physiol Rev.* 1989; 69:179–249. [PubMed: 2643123]
22. Liu Z, Chen Y, Mo R, Chi-chung H, Cheng JF, Mohandas N, Huang CH. Characterization of human RhCG and mouse Rhcg as novel nonerythroid Rh glycoprotein homologues predominantly expressed in kidney and testis. *J Biol Chem.* 2000; 275:25641–25651. [PubMed: 10852913]
23. Liu Z, Peng J, Mo R, Hui CC, Huang CH. Rh type B glycoprotein is a new member of the Rh superfamily and a putative ammonia transporter in mammals. *J Biol Chem.* 2001; 276:1424–1433. [PubMed: 11024028]
24. Ludewig U. Electroneutral ammonium transport by basolateral rhesus B glycoprotein. *J Physiol.* 2004; 559:751–759. [PubMed: 15284342]
25. Ludewig U, von Wiren N, Frommer WB. Uniport of NH<sub>4</sub><sup>+</sup> by the root hair plasma membrane membrane ammonium transporter LeAMT1:1. *J Biol Chem.* 2002; 277:13548–13555. [PubMed: 11821433]
26. Marini AM, Matassi G, Raynal V, Andre B, Cartron JP, Cherif-Zahar B. The human Rhesus-associated RhAG protein and a kidney homologue promote ammonium transport in yeast. *Nat Genet.* 2000; 26:341–344. [PubMed: 11062476]
27. Marini AM, Soussi-Boudekou S, Vissers S, Andre B. A family of ammonium transporters in *Saccharomyces cerevisiae*. *Mol Cell Biol.* 1997; 17:4282–4293. [PubMed: 9234685]
28. Marini AM, Vissers S, Urrestarazu A, Andre B. Cloning and expression of the MEP1 gene encoding an ammonium transporter in *Saccharomyces cerevisiae*. *EMBO J.* 1994; 13:3456–3463. [PubMed: 8062822]
29. Meier-Wagner J, Nolden L, Jakoby M, Siewe R, Kramer R, Burkovski A. Multiplicity of ammonium uptake systems in *Corynebacterium glutamicum*: role of Amt and AmtB. *Microbiology.* 2001; 147:135–143. [PubMed: 11160807]
30. Nakhoul NL, Dejong H, Abdunour-Nakhoul SM, Boulpaep EL, Hering-Smith K, Hamm LL. Characteristics of renal Rhbg as an NH<sub>4</sub><sup>+</sup> transporter. *Am J Physiol Renal Physiol.* 2005; 288:F170–F181. [PubMed: 15353405]
31. Nessler S, Friedrich O, Bakouh N, Fink RH, Sanchez CP, Planelles G, Lanzer M. Evidence for activation of endogenous transporters in *Xenopus laevis* oocytes expressing the *Plasmodium falciparum* chloroquine resistance transporter, PfCRT. *J Biol Chem.* 2004; 279:39438–39446. [PubMed: 15258157]
32. Ninnemann O, Jauniaux JC, Frommer WB. Identification of a high affinity NH<sub>4</sub><sup>+</sup> transporter from plants. *EMBO J.* 1994; 13:3464–3471. [PubMed: 8062823]

33. Quentin F, Eladari D, Cheval L, Lopez C, Goossens D, Colin Y, Cartron JP, Paillard M, Chambrey R. RhBG and RhCG, the putative ammonia transporters, are expressed in the same cells in the distal nephron. *J Am Soc Nephrol*. 2003; 14:545–554. [PubMed: 12595489]
34. Roon RJ, Even HL, Dunlop P, Larimore FL. Methylamine and ammonia transport in *Saccharomyces cerevisiae*. *J Bacteriol*. 1975; 122:502–509. [PubMed: 236281]
35. Sha Q, Lansbery KL, Distefano D, Mercer RW, Nichols CG. Heterologous expression of the Na<sup>+</sup>,K<sup>+</sup>-ATPase  $\gamma$ -subunit in *Xenopus* oocytes induces an endogenous voltage-gated large diameter pore. *J Physiol*. 2001; 535:407–417. [PubMed: 11533133]
36. Shimbo K, Brassard DL, Lamb RA, Pinto LH. Viral and cellular small integral membrane proteins can modify ion channels endogenous to *Xenopus* oocytes. *Biophys J*. 1995; 69:1819–1829. [PubMed: 8580325]
37. Verlander JW, Miller RT, Frank AE, Royaux IE, Kim YH, Weiner ID. Localization of the ammonium transporter proteins RhBG and RhCG in mouse kidney. *Am J Physiol Renal Physiol*. 2003; 284:F323–F337. [PubMed: 12388412]
38. Wall SM. Ammonium transport and the role of the Na, K-ATPase. *Miner Electrolyte Metab*. 1996; 22:311–317. [PubMed: 8933502]
39. Weiner ID, Miller RT, Verlander JW. Localization of the ammonium transporters, Rh B glycoprotein and Rh C glycoprotein, in the mouse liver. *Gastroenterology*. 2003; 124:1432–1440. [PubMed: 12730882]
40. Westhoff CM, Ferreri-Jacobia M, Mak DOD, Foskett JK. Identification of the erythrocyte Rh blood group glycoprotein as a mammalian ammonium transporter. *J Biol Chem*. 2002; 277:12499–12502. [PubMed: 11861637]
41. Westhoff CM, Siegel DL, Burd CG, Foskett JK. Mechanism of genetic complementation of ammonium transport in yeast by human erythrocyte Rh-associated glycoprotein. *J Biol Chem*. 2004; 279:17443–17448. [PubMed: 14966114]
42. Zheng L, Kostrewa D, Berneche S, Winkler FK, Li XD. The mechanism of ammonia transport based on the crystal structure of AmtB of *Escherichia coli*. *Proc Natl Acad Sci USA*. 2004; 101:17090–17095. [PubMed: 15563598]

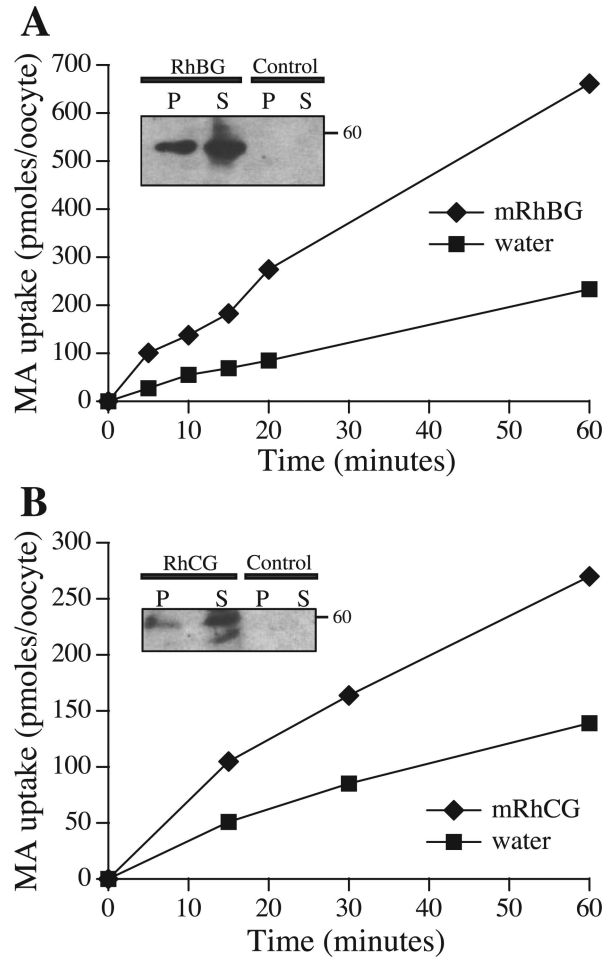


**Fig. 1.**

Expression of kidney RhBG and RhCG and uptake of [ $^{14}\text{C}$ ]methylamine (MA) in *Xenopus laevis* oocytes. RhBG cRNA-injected (A) and RhCG cRNA-injected oocytes (B) have an enhanced rate of uptake in 500  $\mu\text{M}$  total MA compared with water-injected controls. Groups of 6 oocytes were analyzed at each time point, and uptake is reported as pmol/oocyte. mRhCG, mouse RhCG. Data shown are representative of multiple, independent experiments. *Inset*: immunoblot assay of RhBG cRNA- and water-injected control oocytes probed with an affinity-purified peptide-specific antibody (A) and RhCG cRNA- and water-injected control oocytes probed with rabbit anti-peptide antiserum (B). P, membrane pellet; S, supernatant.

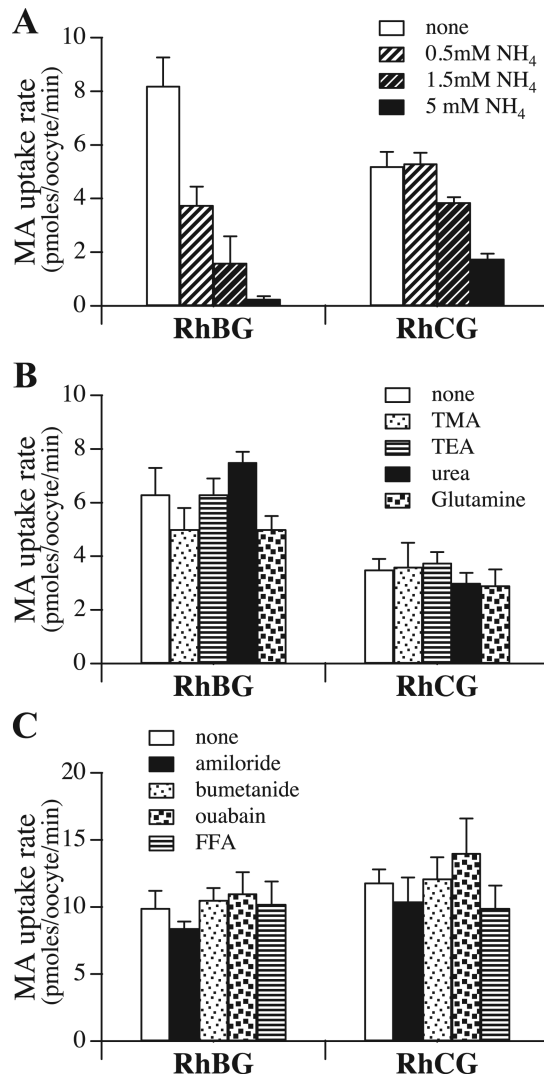


**Fig. 2.** Effect of ammonium, other amine compounds, and transport inhibitors on RhBG- and RhCG-mediated MA transport. **A:** MA uptake rate in the presence of 1.5 mM MA (none) and with addition of 0.5, 1.5, and 5 mM NH<sub>4</sub>Cl reveals that uptake was competitively inhibited by NH<sub>4</sub>Cl. **B:** MA uptake rate in the presence of 500 μM MA (none) and with the addition of 10 mM TMA, TEA, urea, or glutamine. MA uptake was not completed by other amine-containing compounds. **C:** uptake in the presence of 1.5 mM MA (none) was not affected by presence of 1 mM amiloride, 0.1 mM bumetanide, 0.1 mM ouabain, or 0.1 mM fufenamic acid (FFA). Values are means ± SE (*n* = 3) analyzed as groups of 6 oocytes. Rates of uptake observed in water-injected controls have been subtracted.

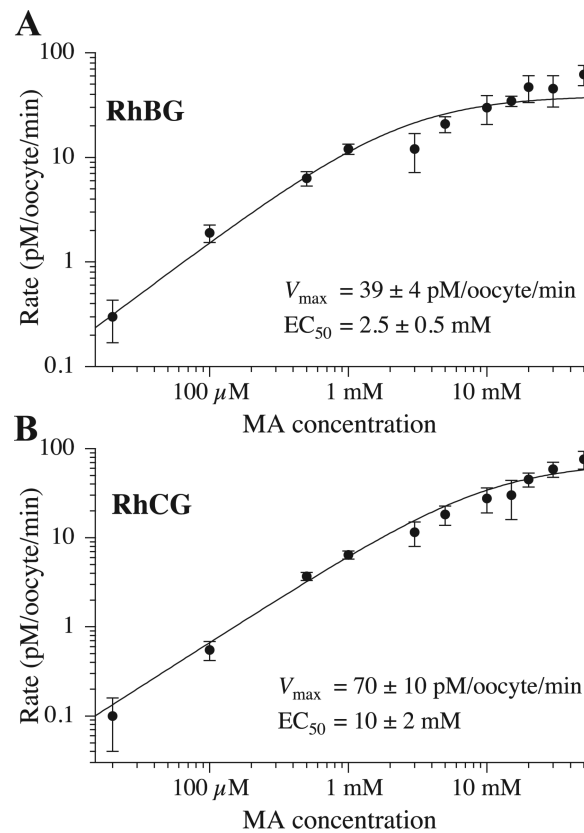


**Fig. 3.** RhBG- and RhCG-mediated transport kinetics. The rate of RhBG (A)-and RhCG (B)-mediated MA/MA<sup>+</sup> uptake was a saturable function of total MA/MA<sup>+</sup>. ● Represent experimental data, and the curve represents the Michaelis-Menten fit with the tabulated parameters. The EC<sub>50</sub> (*K<sub>m</sub>*) for RhBG was 2.5 mM compared with an EC<sub>50</sub> (*K<sub>m</sub>*) for RhCG of ~10 mM. Values are means ± SE of groups of 6 oocytes (*n* = 5 to 15). Rates of uptake observed in water-injected controls have been subtracted.



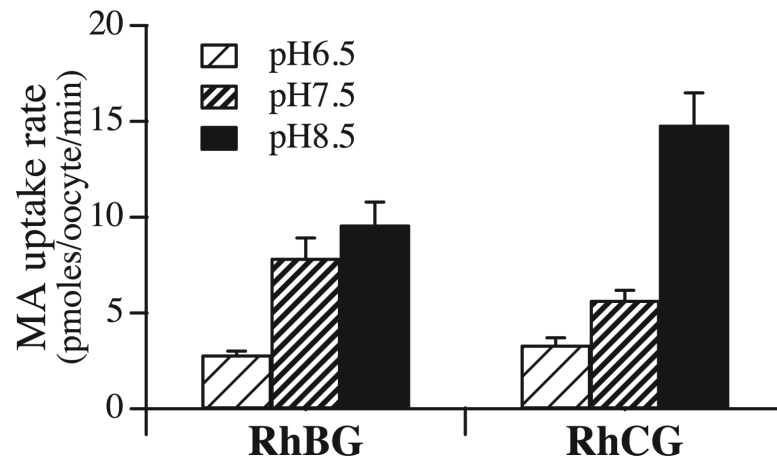


**Fig. 4.** RhBG- and RhCG-mediated MA/MA<sup>+</sup> uptake in buffers at various pH. Uptake is significantly increased in RhBG and RhCG cRNA-injected oocytes at alkaline pH values. Data shown are in the presence of 1.5 mM total MA/MA<sup>+</sup>. Values are means  $\pm$  SE of groups of 6 oocytes ( $n = 5$ ). Rates of uptake observed in water-injected controls have been subtracted.

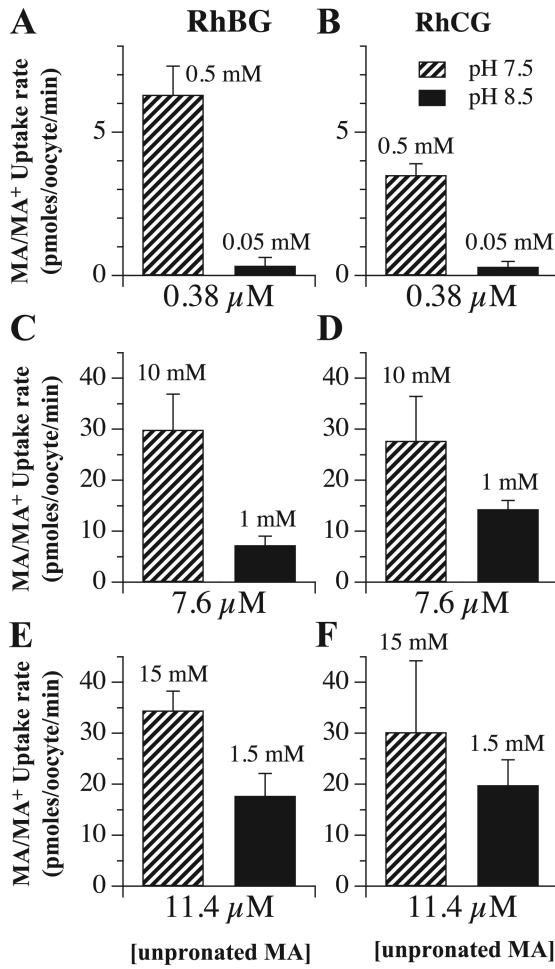


**Fig. 5.** RhBG- and RhCG-mediated MA/MA<sup>+</sup> uptake as a function of unpronated MA. Each graph shows rates of MA/MA<sup>+</sup> uptake by RhBG or RhCG in the presence of a fixed concentration of the unpronated species MA (0.38, 7.6, or 11.4 μM). Each concentration was generated with a 10-fold difference in total (protonated and unpronated) concentration (as indicated above the bars in the graph) at the pH values indicated. Values are means ± SE of groups of 6 oocytes (*n* = 3). Rates of uptake observed in water-injected controls have been subtracted.

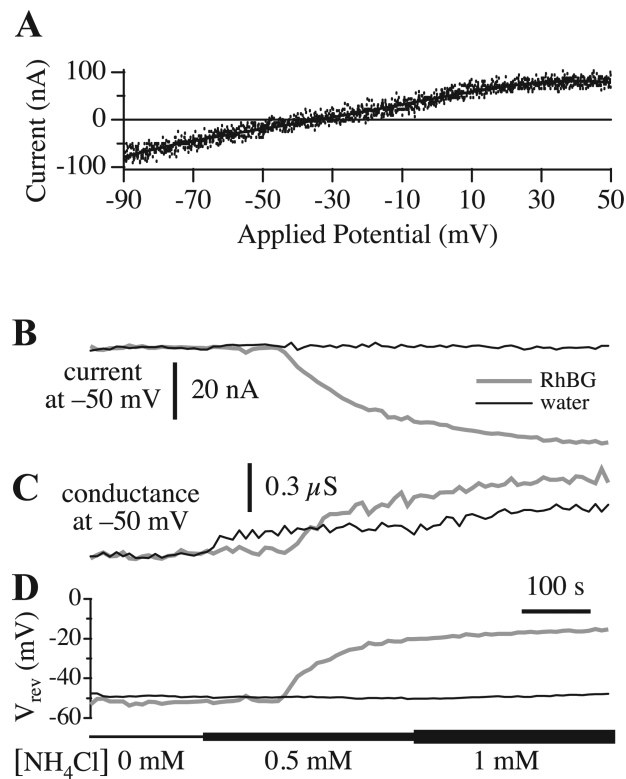


**Fig. 6.** Two-electrode voltage clamp (TEV). *A*: whole oocyte current-applied transmembrane potential relationship obtained during one voltage ramp for a RhBG cRNA-injected oocyte perfused with 0.5 mM  $NH_4Cl$  bath solution. Dots represent individual  $I_m$  measured at various  $V_m$  during the voltage ramp. The solid line is the polynomial fitted to the data (dots). *B*: whole oocyte trans-membrane currents at -50 mV. *C*: slope conductance at -50 mV. *D*: reversal potential ( $V_{rev}$ ) for a RhBG-expressing (gray line) and a water-injected control (black line) oocyte perfused with solutions containing 0, 0.5, and 1 mM  $NH_4Cl$ .

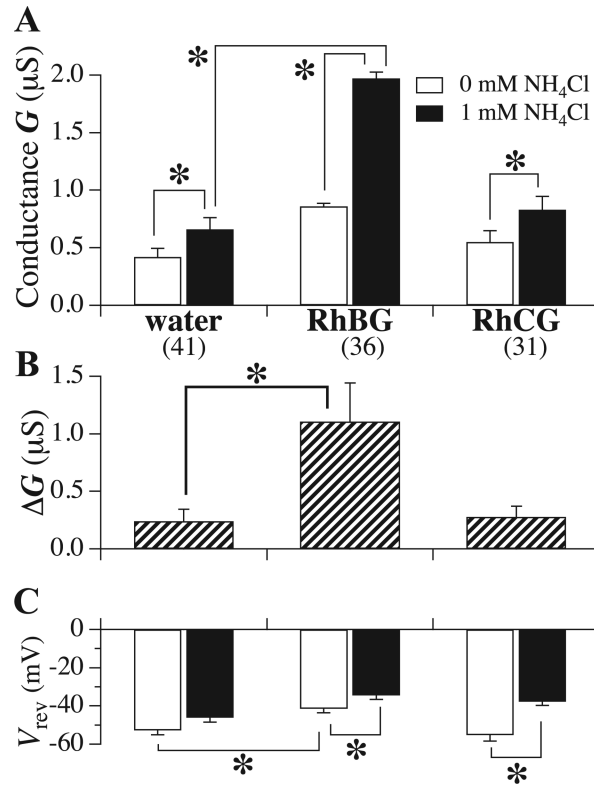


**Fig. 7.** Effects of RhBG and RhCG expression in oocytes on TEV results. *A*: mean whole oocyte conductance ( $G$ ) at  $-50$  mV observed in the presence of 0 (open bars) and 1 (filled bars) mM  $\text{NH}_4\text{Cl}$  in the perfused bath solutions. *B*: changes in mean whole oocyte conductance at  $-50$  mV stimulated by 1 mM  $\text{NH}_4\text{Cl}$ . *C*: mean reversal potentials in the presence of 0 and 1 mM  $\text{NH}_4\text{Cl}$  for water, RhBG- and RhCG-expressing oocytes. Number of each type of oocyte used for averaging is indicated by numbers in brackets. \*Statistically significant difference ( $P < 0.05$ ) between pairs of quantities linked by square brackets.

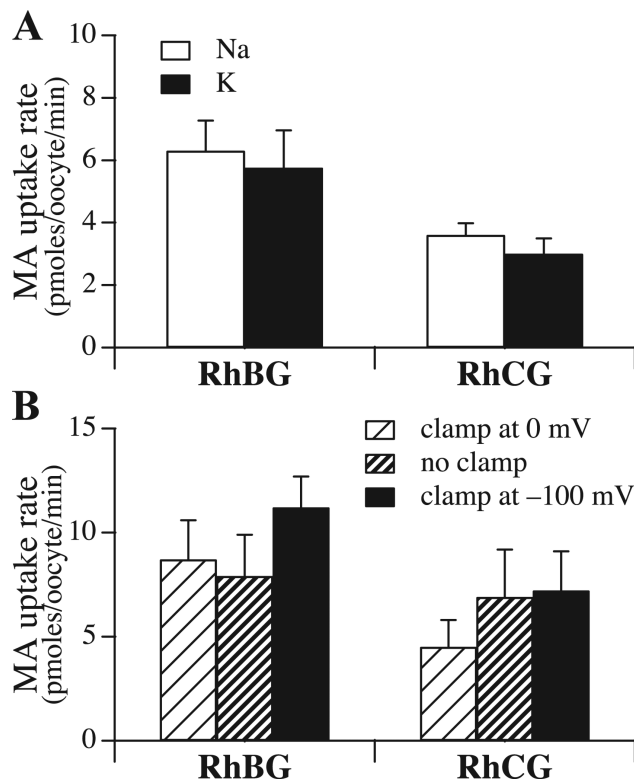


**Fig. 8.** Effect of membrane potential on transport. *A*: MA/MA<sup>+</sup> uptake in standard Na<sup>+</sup> buffer (open bars) and in buffer in which all Na<sup>+</sup> was replaced with K<sup>+</sup> (filled bars). Values are means  $\pm$  SE ( $n = 3$ ) of groups of 6 oocytes. *B*: MA/MA<sup>+</sup> uptake in individual oocytes whose transmembrane potential is clamped at 0 or -100 mV, or not clamped. Values are means  $\pm$  SE ( $n = 10$ ). Rates of MA uptake observed in water-injected control oocytes have been subtracted.

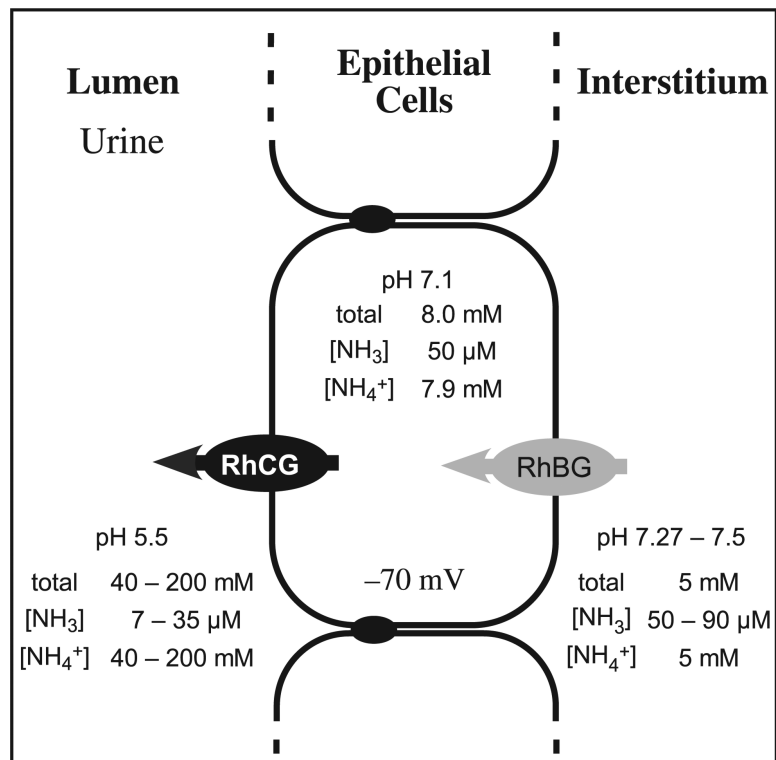


**Fig. 9.**

Diagrammatic representation of the kidney collecting duct showing the location of RhBG and RhCG and indicating the local medullary pH and the approximate local concentration of total ammonia (both  $\text{NH}_4^+$  and  $\text{NH}_3$ ),  $\text{NH}_3$ , and  $\text{NH}_4^+$ . RhCG is at the apical membrane facing the very acidic lumen, and RhBG is located in the basolateral membrane, at the interface with the interstitium. The proposed direction of net transport of  $\text{NH}_3$  by RhBG and RhCG is indicated by the arrows.